Single-molecule pump-probe experiments reveal variations in ultrafast energy redistribution

E. M. H. P. van Dijk, J. Hernando,[a] M. F. García-Parajó, and N. F. van Hulst[b]
Applied Optics Group, Department of Science and Technology and MESA+ Institute for Nanotechnology, University of Twente, P.O. Box 217, 7500AE Enschede, The Netherlands

(Received 18 February 2005; accepted 2 May 2005; published online 15 August 2005)

Single-molecule pump probe (SM2P) is a novel, fluorescence-based technique that allows the study of ultrafast processes on the single-molecule level. Exploiting SM2P we have observed large variations (from 1 ps to below 100 fs) in the energy redistribution times of chemically identical molecules in the same sample. Embedding the molecules in a different matrix or changing the excitation wavelength does not lead to significant changes in the average redistribution time. However, chemically different molecules exhibit different characteristic redistribution times. We therefore conclude that the process measured with the SM2P technique is dominated by *intramolecular* energy redistribution and not *intermolecular* transfer to the surrounding matrix. The matrix though is responsible for inducing conformational changes in the molecule, which affect the coupling between electronic and vibrational modes. These conformational changes are the main origin of the observed broad distribution of redistribution times. © *2005 American Institute of Physics*. [DOI: 10.1063/1.1940567]

I. INTRODUCTION

Many important optical processes in both natural and synthetic molecular systems occur on a femtosecond time scale. One example of such a process is the rapid transfer of energy from one excited chromophore to another in light harvesting complexes[1,2] or synthetic molecular coupled systems such as conjugated polymers.[3] Also intramolecular processes within large, complex chromophores (under ambient conditions) occur on a femtosecond time scale.[4] In general all these fast processes are studied using time-resolved pump-probe techniques. The system under study is brought into a specific state by a short, pump pulse and after some time the evolution from this state is probed by a second probe pulse. Over the last decades a large number of different implementations of this general scheme have been presented,[5–10] yielding very detailed information on the ultrafast processes inside molecules[10] and interactions with the surroundings.[5–7] These various techniques, however, have one major drawback: they all yield the ensemble averaged response of the whole system under study. Furthermore, only processes that can be optically synchronized can be followed. For instance, binding and unbinding events or conformational changes cannot be followed in real time since these changes occur at different times for different molecules in the experiment.[11]

On the other hand, in recent years it has become possible to study individual molecules one at a time and follow their behavior in time. First experiments were performed at cryogenic temperature, where the narrow absorption linewidth of the molecules allowed molecules to be selected in the spectral domain.[12,13] Later experiments at room temperature used the ultrahigh resolution of near-field microscopes to select molecules in space.[14,15] Nowadays, using confocal and wide-field microscopy techniques, the observation of single molecules has become routine in studying physical,[16–24] chemical,[25–28] and biological[11,29–37] systems. All these studies show that chemically identical molecules generally exhibit widely different behaviors on all studied time scales due to variation in the local surroundings. However, so far the time scales available in single-molecule experiments have been limited, since the experiments all rely on detecting the Stokes-shifted fluorescent photons. Fluorescence is a relatively slow process occurring usually on a nanosecond time scale. Resonant detection with a faster time response is only possible under cryogenic conditions were the cross sections are large enough.[38] To address faster processes at room temperature it is therefore necessary to implement a technique that combines the time resolution of pump-probe methods with the sensitivity of single-molecule detection. The pioneering work by Dyba and Hell[39] on the stimulated emission depletion (STED) was a first example of combining single-molecule sensitivity and a pump-dump scheme. In these experiments a molecule was excited with a pulse and a second picosecond pulse was used to stimulate all vibrational modes down to the ground state, thereby reducing the fluorescence. STED has been used to increase the resolution of the fluorescence microscopy[39] and measure the absorption cross section of the excited state.[40] However, these elegant experiments did not yield any time-resolved information.

We recently presented the first *femtosecond time-resolved* single-molecule pump-probe (SM2P) experiments[41] on individual and excitonically coupled molecules at room temperature. Here, the principle of operation of the SM2P technique is described in detail, providing at the same time a

[a]Present address: Departamento de Química, Universidad Autònoma de Barcelona, 08193 Cerdanyola del Vallès, Spain.
[b]Electronic mail: n.f.vanhulst@utwente.nl

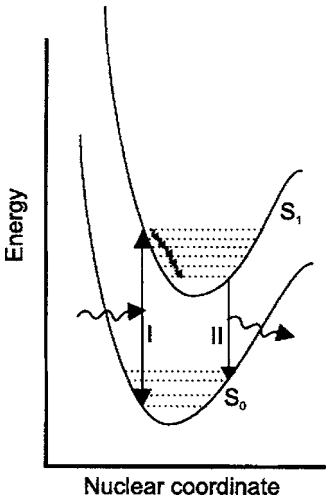

FIG. 1. Schematic representation of some of the energy levels in a molecule. The solid lines indicate the potential of the electrons in the ground (S_0) and first excited states (S_1), and the dotted levels represent the vibrational modes in the molecule. The arrows indicate the stimulated excitation (deexcitation) (I) of the molecule to (from) the excited state by the laser and the spontaneous decay (II) back to the ground state.

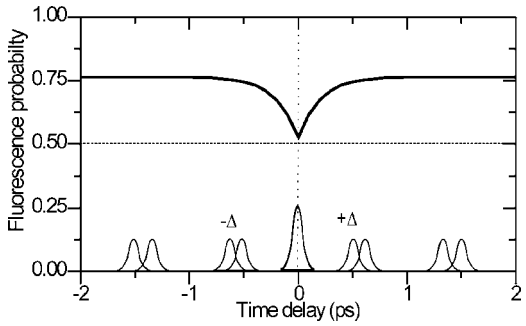

FIG. 2. Schematic description of the fluorescent response of the molecule upon excitation with two saturating pulses with variable delay times. For zero delay the fluorescence probability is 0.5. For delay times longer than the vibrational redistribution time the fluorescence probability increases to 0.75.

description of the underlying mechanism. We have applied the method to systematically study the effect of both the surrounding matrix and the excitation wavelength on the ultrafast response of individual molecules. Finally, we discuss the nature of the process being probed in these novel single-molecule experiments.

II. THE SM2P CONCEPT

We have devised a method that yields ultrafast information while still relying on fluorescence detection, thus circumventing the time limitations of standard fluorescence-based single-molecule experiments. The method exploits the balance between stimulated emission and absorption to provide an insight in the ultrafast processes occurring just after excitation. Figure 1 schematically depicts two of the electronic energy levels in a molecule, the ground state S_0 and the first excited state S_1, both dressed with a large number of vibrational states (dotted lines). In a perfect two-level system a molecule that is initially in the ground state can be transferred to the excited state by a field with a frequency that corresponds to the energy difference between the ground and excited states. However, once in the excited state, the same field will have an equal probability to return the molecule to the ground state, via stimulated emission. The molecule will therefore alternate between the excited and ground states, leading to so-called Rabi oscillations. Therefore, the probability of finding the molecule in the excited state oscillates between zero and one. By switching the laser off at the right point in this cycle, using a so-called π pulse, it is possible to obtain a probability near unity of finding the molecule in the excited state.[42]

When the system cannot be described as a perfect two-level system, the Rabi oscillations will be damped due to dephasing between the excitation field and the molecule. Moreover, due to vibrational coupling other states will also start to be populated. As a result, after some time the probability of finding the molecule in the excited state becomes 0.5. For large organic molecules under ambient conditions the fluorescence linewidth is very broad ($\sim$50 nm); hence, the dephasing is very rapid ($\sim$20 fs) and the Rabi oscillations are superdamped.[18,43] In this situation, the probability of finding the molecule in the excited state following an intense short Fourier-limited laser pulse will never exceed 0.5 and the molecule will be saturated. When the molecule ends up in the excited state after the laser field is switched off, the only way to return to the electronic ground state is by emitting a fluorescent photon (assuming a quantum yield of unity). However, since the molecule is initially in a state that has some excess vibrational energy, it can first lose some of this energy by relaxing to lower states of the first electronic excited state. The emitted fluorescent photon is therefore red-shifted.

The SM2P technique relies on the fact that once a first saturating pulse has interacted with the molecule, a second equally intense pulse interacting at the same time will not increase the probability of the molecule ending up in the excited state. This second pulse will have an equal probability of stimulating the molecule up or down. As a result, the chance of finding the molecule in the excited state after the two pulses have passed remains 0.5, as depicted in Fig. 2. Let us now consider the case when the two pulses do not coincide in time. After the first laser pulse passed, the molecule can either be in the excited state or in the ground state. We first consider the situation where the molecule ended up in the excited state. If the molecule has had time to redistribute some of its energy to different vibrational modes before the second pulse impinges, the molecule will be in a state where it cannot interact with the laser light.[44,45] In this case, the second pulse will not be able to stimulate the molecule down to the ground state, leaving the molecule in the excited state from where it must emit a fluorescent photon in order to return to the ground state. However, if the molecule was left in the ground state by the first pulse, the second pulse will have another chance of bringing the molecule into the excited state. Again, this will only occur half of the time. The net effect of a second saturating pulse impinging at some time after the molecule relaxed will be an increase of the chance that the molecule is left in the excited state to 0.75. By varying the delay between the two saturating pulses it

becomes possible to study the time scale of the onset of the redistribution of the initially excited vibrational modes to other vibrational modes until the molecule is no longer accessible to the incoming laser light. Figure 2 schematically depicts the response of the molecule as the delay between two saturating pulses is varied. As shown, the fluorescence probability is 0.5 at zero delay and increases for longer pulse delays, leading to a clear dip in the fluorescence at $\Delta\tau=0$ as the delay time is scanned.

III. SM2P: EFFECT OF PULSE LENGTH AND EXCITATION CONDITION

In a real experiment the pulses will not be infinitely short. To investigate the effects of finite pulse length on the expected signal, we introduce a simple numerical model. The molecule is considered as a three-level system. Coherent effects are ignored since dephasing at room temperature is much faster than the pulse length used to excite the molecule. The ground state (S_0) is coupled to the initially excited state S_1 via the laser light. The state S_1 has a decay rate k_{er} to a state S_1' which is no longer coupled to the ground state by the laser light. The state S_1' decays spontaneously with a rate of k_f back to the ground state upon emission of a fluorescent photon. The system can then be described with the following coupled differential equations:

$$\frac{dN_0(t)}{dt} = -I(t)\sigma(N_0(t)-N_1(t)) + k_f N_1'(t),$$

$$\frac{dN_1(t)}{dt} = I(t)\sigma(N_0(t)-N_1(t)) - k_{er}N_1(t), \tag{1}$$

$$\frac{dN_1'(t)}{dt} = k_{er}N_1(t) - k_f N_1'(t),$$

where σ is the absorption cross section (assumed to be equal in the excited and ground states) and $N_0(t)$, $N_1(t)$, and $N_1'(t)$ are the time-dependent populations in the three different states. $I(t)$ is the laser intensity at time t. The two pulses are modeled as Gaussian intensity profiles with a certain width and a delay between them. The differential equations are numerically integrated over a time interval from before the first pulse until after the second pulse. The total population that passes through state S_1' is a measure for the fluorescence probability since the system has to return to the ground state via fluorescence from this state.

In Fig. 3 the calculated fluorescence probability is plotted as a function of the time delay between the two pulses for a k_{er} corresponding to a redistribution time of 150 fs. The different symbols indicate data simulated under different "experimental" conditions. In all cases we find a clear reduction in the fluorescence probability at zero time delay.

In our simulations we have investigated both the effect of the pulse length and peak intensity on the recovery of the redistribution times. First, we have considered pulses with lengths both shorter (90 fs indicated by circles) and longer (280 fs indicated by squares, triangles, and stars) than the redistribution time (150 fs). Next, we have investigated peak intensities below, equal, and above the saturation intensity.

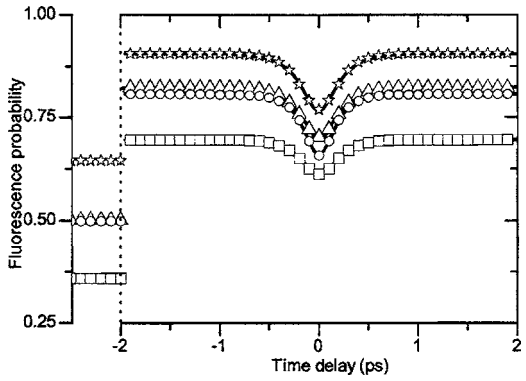

FIG. 3. The simulated fluorescence probability of a single molecule with a redistribution time of 150 fs when varying the delay between two femtosecond pulses. Different conditions have been simulated. The (○) indicates a pulse duration of 90 fs with a peak intensity such that it exactly saturates the molecule. For pulses of 280 fs the intensity was varied. The case where the intensity is such that the molecule is exactly saturated is indicated by (△). The (□) and (⋆) show the results when half and double the saturation power is used, respectively. The response of the molecule under illumination of a single pulse is depicted on the left side of the graph. The solid lines show fits through the points using function Eq. (2), yielding in all cases the correct redistribution time of 150±5 fs.

The pulses that exactly saturate the system (circles and triangles) lead to a fluorescence probability of 0.5 when a single pulse is present (see the left side of the plot). The signal is lower (squares), when each of the pulses is not intense enough to fully saturate the system. For pulses longer than the redistribution time, a higher intensity (stars) will lead to slightly more than 0.5 fluorescence probability.

Clearly for finite pulse lengths the response is convoluted by the pulse width. However, it is also clear that the dip is still visible and the underlying redistribution time can be recovered by simply deconvoluting the measured response with the pulse length. The response for an infinitely short pulse can be described as

$$I(t) = (I_{\mathrm{dip}} - I_{\mathrm{long}}) * e^{(-1/\tau_{er})|t|} + I_{\mathrm{dip}}, \tag{2}$$

where $I(t)$ is the fluorescence intensity as a function of the delay time, I_{dip} is the intensity at delay zero, I_{long} is the fluorescence intensity at long time delay, and τ_{er} is the redistribution time ($=1/k_{er}$). Before fitting the data, Eq. (2) is convoluted with a Gaussian function to account for the finite width of the pulses. In the four different cases we find τ_{er} within 3% of the 150 fs we used as input in the simulation. This indicates that the redistribution time is recovered with confidence even for times shorter than the pulse width. A deviation in the chosen pulse length will only introduce a systematic error. Thus, any variation found between molecules measured with the same pulse length will be due to a variation in the underlying τ_{er}. It is important to note that for the fitting of the simulations in Fig. 3 the actual degree of saturation of the molecules (for instance due to spectral or orientational differences) is not critical in the determination of τ_{er}. Finally, it should also be noted that the ratio between I_{dip} and I_{long} does depend on the excitation efficiency and should therefore not be used to extract information on the redistribution time.

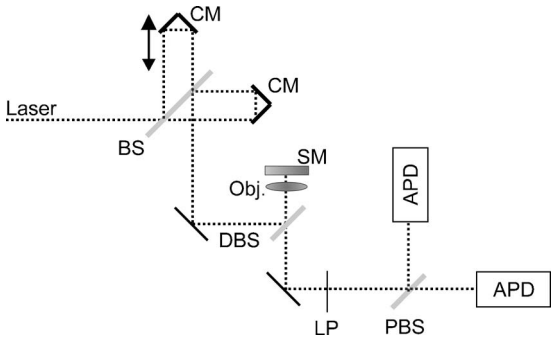

FIG. 4. SM2P experimental setup used in the experiments. Short laser pulses are split into two different branches using a beam splitter (BS) and are recombined on the same beam splitter after reflecting the two beams by two corner mirrors (CMs). One of the mirrors can be moved, varying the delay between the pulses. The light is made circularly polarized before entering the confocal microscope. After reflection from the dichroic beam splitter (DBS) the pulse train is focused with a high NA objective (Obj.) onto the sample. The fluorescence light from the single molecules (SMs) embedded in the sample is collected with the same objective, passes through the dichroic beam splitter and a long pass (LP) filter. The light is then split in two orthogonal polarizations by a polarizing beam splitter (PBS) and finally focused on two avalanche photodiodes (APDs).

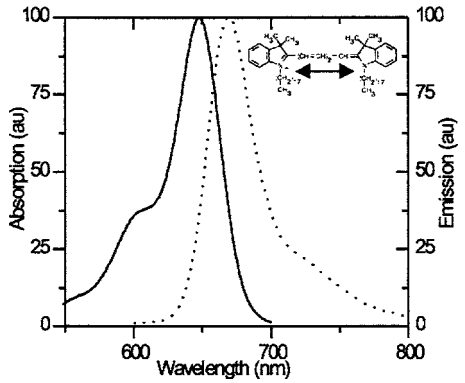

FIG. 5. Bulk absorption and emission spectra of DiD. The inset shows the molecular structure of the molecule. The dipole direction is indicated by the arrow.

IV. EXPERIMENTAL DETAILS

The experimental SM2P setup is depicted in Fig. 4. The laser system consists of diode-pumped mode-locked 80 MHz Ti:saphire laser (Spectra Physics, Tsunami) pumping a tunable optical parametric oscillator (OPO) (Spectra Physics, Opal) that is finally frequency doubled to yield Fourier-limited pulses in the visible. The pulse duration after the frequency doubler is measured by a background-free intensity autocorrelation technique yielding a full width at half maximum (FWHM) of the pulse amplitude of 280 ± 10 fs. A pulse picker (Spectra Physics) was used to reduce the repetition rate of the pulses. Since fluorescent molecules undergo an irreversible transition to a dark state after a finite number of photocycles, it is important to select a pulse rate that allows for both (i) enough time to scan the delay between the pump and probe pulses prior to photobleaching, and (ii) a good signal-to-noise ratio. With a repetition rate of 500 kHz, molecules could be studied for up to tens of seconds. The selected pulses are then split by a beam splitter and via two corner mirrors recombined on the same beam splitter. This configuration ensures that both beams will run parallel and thus will be focused at the same position on the sample by the objective. One of the corner mirrors was placed on a translation stage driven by a computer-controlled stepper motor (Oriel, Encoder Mike). A computer-controlled shutter was used to block the light in one of the arms. Circularly polarized light was used in order to achieve equal excitation conditions for molecules with different in-plane orientations. Before entering the microscope a small fraction of the light was split off to monitor the excitation conditions with a photodiode. The pulse train then entered the sample scanning confocal microscope. The light was reflected from a dichroic mirror (Omega Optical, Inc.) and focused with a high numerical aperture (NA) objective (Zeiss, 1.4 NA oil) onto the sample. Fluorescence was collected with the same objective and passed through a long-pass filter (Omega Optical, Inc.). The fluorescence was split into two orthogonal polarization components with a polarizing beam splitter and focused onto two avalanche photodiodes (Perkin and Elmer, SPAPD-AQR-14). This arrangement allows the in-plane emission dipole of the molecule to be measured. It was found that under the experimental conditions the molecules were fixed and did not show any rotational diffusion. In the analysis of the ultrafast times the signals from both detectors were therefore added to improve the signal-to-noise ratio. The sample scanning, data acquisition, and the position of the delay line are all controlled by a custom-made software.

Several different types of molecules were studied: DiD (1,1′-dioctadecyl-3,3,3′,3′-tetramethylindodicarbocyanine, Molecular Probes, see Fig. 5), perylene(tetratbutylphenoxy-perylene diimide), Cy3.5 (DNA Technology A/S) and Atto590 (ATTO-TEC GmbH). The DiD and perylene samples were prepared by dissolving $\sim10^{-9}M$ of the chromophore with 0.5% poly(methyl methacrylate) (PMMA) or zeonex in toluene and spin coating these solutions on cover slips. These concentrations lead to uniform films with a thickness of around 20 nm, and with less than 1 chromophore per μm^2. Before spin coating the cover slips were O_2-plasma etched for 6 min to remove any organic pollution. Blank PMMA and zeonex samples were thoroughly checked before each experiment making sure that no fluorescent pollution was present.

The Cy3.5–DNA and Atto590 samples were prepared by dissolving $\sim5\times10^{-9}M$ of the molecules in 1% poly vinyl alcohol (PVA)/water solutions and then spin coating on O_2-plasma-cleaned glass cover slips. The samples were also prepared by dissolving $\sim5\times10^{-9}M$ of the molecules in water and directly spinning these solutions on the cleaned glasses.

We started our experiments with the study of the ultrafast processes of DiD. Before performing the actual pump-probe experiments, the pulse powers needed to saturate the molecule were determined. To that end, a large number of individual molecules were measured under ever increasing excitation powers. We found that 2 pJ per pulse (repetition rate of 500 kHz, average power density of ~1.6 kW/cm^2) was enough to saturate the majority of the molecules, yielding count rates of ~14 kcounts/s. Taking into account the

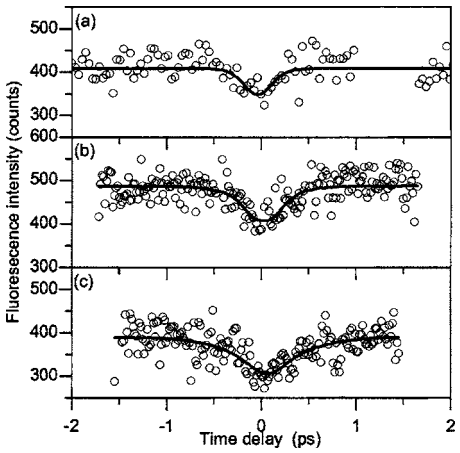

FIG. 6. Three delay traces obtained on single DiD molecules in a PMMA matrix. The fluorescence signal is plotted vs the delay time between the pulses. A clear reduction in the fluorescence at $\tau=0$ can be observed in all three traces. Differences in the depth and width of the dips can clearly be observed. Taking into account the finite pulse length we recover redistribution times of 95±50, 160±30, and 350±25 fs for traces (a), (b), and (c), respectively.

detection efficiency of ~5%, this count rate indeed corresponds to one photon emitted for each two laser pulses and thus confirming saturation.

Each experiment started by imaging a 10×10 μm^2 area of the sample with single-pulse excitation, enabling the selection of well-separated single molecules. Next, selected molecules were repositioned one by one in the focus of the objective using a lateral position feedback on the scanner. To verify that the molecule was indeed near saturation we first recorded its fluorescence for 0.5 s with only one pulse present. The second pulse was then added and the delay line was scanned with a constant speed of 100 μm/s over a distance of ~1 mm. This corresponds to a change in the delay between the pulses from ~−3 to ~+3 ps, with a constant speed of ~666 fs/s. As the delay line was scanned, the fluorescence intensity was measured with an integration time of 1 ms. At the end of the delay run one of the pulses was shortly blocked to verify once more the response of the molecule under single-pulse excitation. Finally the delay mirror was moved in the opposite direction. This cyclic process was continuously repeated until permanent photodegradation of the molecule occurred, thus obtaining maximum information from each molecule.

V. RESULTS

Figure 6 shows as an example SM2P traces for three different DiD molecules in the same PMMA matrix. In all cases the molecules were excited at the wavelength of the absorption maximum: 647 nm (see Fig. 5). The delay between the exciting pulses was varied from −2 to +2 ps while the fluorescence intensity was continuously recorded. All traces clearly show the expected reduction in the fluorescence intensity at zero delay. Surprisingly, the width of the dips is clearly different for the three molecules. By fitting Eq. (2) (solid line) to the data the decay times for the different molecules can be determined. We recover times of 95±50, 160±30, and 350±25 fs for molecules (a), (b), and (c), respectively. The accuracy of the fit is fundamentally limited by the number of counts detected and the shot noise related to the photon counting nature of the detected signal. Monte Carlo simulations were performed to determine the accuracy of the fits based on the detected number of counts and the actual value of τ_{er}. Under our experimental conditions τ_{er} could be determined down to about 50 fs, with an accuracy of ±50 fs below 100 fs, and better than ±35 fs for values above 150 fs.

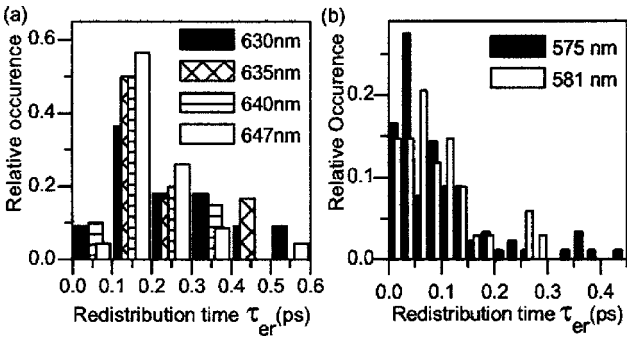

FIG. 7. (a) Histogram of the different redistribution times found for DiD in PMMA at four different excitation wavelengths. (b) Histogram of the times found for perylene in PMMA at two different excitation wavelengths.

To study this ultrafast process in DiD in more detail, we lowered the excitation wavelength with the aim of exciting the molecules to higher vibrational states. A large number of molecules were studied at wavelengths of 630, 635, 640, and 647 nm, corresponding to 970, 842, 716, and 398 cm^{-1} above the lowest excited state, respectively (see Fig. 5). The crossing point between the absorption and the emission spectrum was taken as the position of the S_0-S_1 origin. Figure 7(a) shows the occurrence histograms of the recovered τ_{er} for different excitation wavelengths. For all wavelengths studied the histograms are rather broad and have similar peak values. The peak positions and the widths from a Lorentzian fit to the histograms are plotted in Fig. 8 as a function of the energy above the lowest excited state.

Similar distributions were also obtained for DiD molecules embedded in a zeonex matrix. The peak value and width of the distribution for two different excitation wavelengths are also included in Fig. 8. From this figure it is clear that the peak value of the τ_{er} distribution is around 180 fs for DiD independently of the matrix and the excitation wavelength.

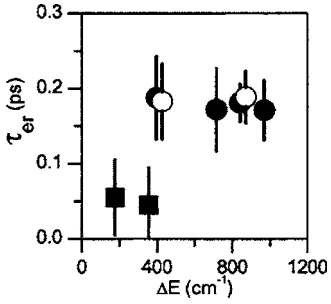

FIG. 8. The peak value and width from a Lorentzian fit of the distributions shown in Figs. 7(a) and 7(b) vs the energy difference with respect to the lowest excited state for DiD (circles) and perylene (squares) in PMMA (solid symbols) and in zeonex (open symbols).

To compare the τ_{er} values found in DiD with those on another type of molecule, experiments were performed on a perylene derivative embedded in PMMA. In Fig. 7(b) the results are plotted for perylene excited at 575 and 581 nm, corresponding to 355 and 175 cm^{-1} above the origin, respectively. Similarly as to the results found for DiD, we also find large variations in the recovered τ_{er} values, with a peak value around ~50 fs, as also shown in Fig. 8. These times are clearly shorter than those recovered for DiD in the same matrix.

VI. DISCUSSION

The observation of such short times independent of the matrix while depending strongly on the type of molecule is indicative for an intramolecular process, responsible for the redistribution of the vibrational energy. Most ensemble studies on large organic chromophores attribute these ultrafast time scales to intramolecular vibrational redistribution (IVR).[44–46] Yet, hole burning experiments in *a*-polar supercooled liquids have shown that also ultrafast, subpicosecond contributions to the relaxation times can be mediated by coupling to the matrix, which are attributed to phonon-modulated interactions.[47,48] In our case, however, the lack of dependence on the matrix for the found redistribution times indicates that the measured process is rather an intramolecular rather than an intermolecular process.

Our single-molecule approach yields for the first time the distribution of the energy redistribution times. Since all molecules are in principle chemically identical one would expect a very narrow distribution of redistribution times for such an intramolecular process. On the other hand, it is well known from single-molecule experiments that slightly different molecular conformations can be induced by the nanoenvironment.[25,28] For perylenedimide it has been shown that small changes in the twist angle between the naphthalene units can lead to large variations in the vibronic progression of the fluorescence emission spectrum.[25] These variations in the vibronic spectra are indicative of large variations in the coupling between the electronic and vibrational modes, which could be responsible for variations in the experimentally recovered energy redistribution times.

For $DiIC_{12}$, a carbocyanine dye related to DiD spectral variations of a few hundred wave numbers have been observed in PMMA[20] and on glass.[49] Therefore, it is not too surprising that no systematic change in the energy redistribution time is observed when changing the excitation frequency by 600 cm^{-1} (see Fig. 8). The heterogeneity in the transition energy from molecule to molecule will lead to a similar set of vibrations being probed in all cases. If the energy redistribution would be dependent on the initially excited vibration, the heterogeneity in transition energies will largely obscure this dependence. A SM2P experiment where the fluorescence spectrum is simultaneously obtained should shed light on the relation between the excited vibration and the observed redistribution time.

On the other hand the dynamics of the variations of the redistribution times on the same molecule might be influenced by the matrix and the temperature. However, the experiments reported in this study were performed at room temperature, well below the glass transition temperature of the matrices investigated, and thus only very slow changes in conformation are expected.[28] In fact, no variations of the redistribution time on individual molecules were observed on the scale of tens of seconds probed in this experiment.

TABLE I. Overview of the experimental conditions used for the SM2P experiments on different dyes and the number of photon counts before photodissociation

Dye	Matrix	Excitation wavelength (nm)	Rep. rate	Photon counts until photobleaching
Cy3.5–DNA	PVA	572	500 kHz	$\sim 3\times10^4$
Cy3.5–DNA	Air	572	500 kHz	$\sim 3\times10^4$
Atto590	PVA	572	500 kHz	$\sim 5\times10^4$
Atto590	Air	572	500 kHz	$\sim 3\times10^4$
DiD	PMMA	630–647	1 MHz	$\sim 1\times10^5$
Perylene	PMMA	575–581	1 MHz	$\sim 3\times10^5$

VII. SM2P: GENERAL APPLICABILITY

To show the general applicability of our method to more photolabile dyes, we also performed SM2P experiments on two other dyes, namely, Cy3.5 and Atto590. The cyanine dye Cy3.5 is extensively used in single-molecule experiments due to the easy coupling to DNA and proteins. Different dyes from the Cy family form good pairs in fluorescence resonance energy-transfer (FRET) experiments. These experiments are applied to the study of DNA–protein and protein–protein interactions. We have performed SM2P experiments on Cy3.5–DNA, a 90-nucleotide oligomer where the Cy3.5 is attached to the 5′ end through a three-carbon linker. Absorption and emission maxima of Cy3.5 are at 581 and 596 nm, respectively.

Atto dyes are water soluble chromophores commonly used as fluorescent labels for a large variety of biomolecules, specifically to label DNA, RNA, and proteins. We selected Atto590, a rhodamine derivative with absorption and emission maxima at 595 and 624 nm, respectively.

The SM2P experimental conditions for all dyes are summarized in Table I, where the DiD and the perylene experiments are included for comparison. All experiments were performed under ambient conditions. Both Cy3.5–DNA and Atto590 were excited at 572 nm. An energy of ~2.1 pJ per pulse at 500 kHz repetition rate ($I_{avg}\sim 2$ kW/cm^2) was enough to saturate most molecules (determined by comparing the fluorescence signal from a single-pulse excitation to that of two-pulse excitation). All dyes showed discrete photobleaching typically within some seconds. The average number of detected photon counts varied from $\sim 3\times10^4$ for Cy3.5–DNA and Atto590, up to $\sim 3\times10^5$ for perylene.

For the experiments on Cy3.5 and Atto590 the delay line was scanned at 200 μm/s, allowing a delay from −2 to +2 ps to be measured in 3 s, sufficient to determine the ultrafast decay of all fluorophores studied.

Figure 9 shows examples of measured traces for the two dyes studied under different conditions, i.e., directly on glass and embedded in PVA. All traces show the characteristic dip

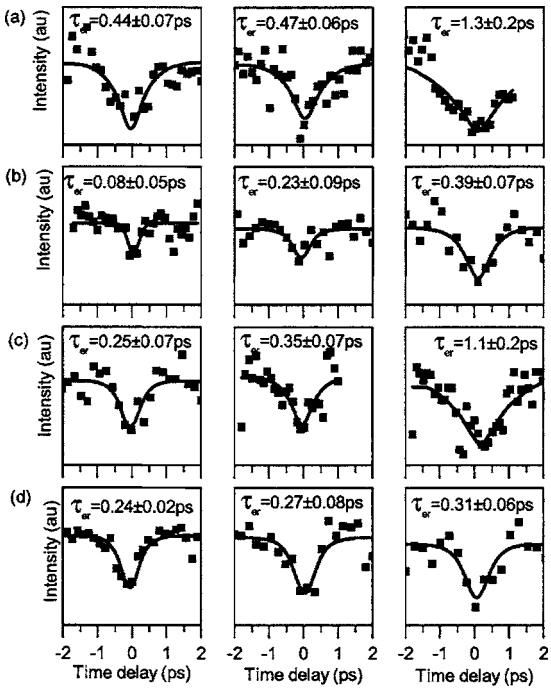

FIG. 9. SM2P traces on Cy3.5 in air (a) and PVA (b) and Atto590 in air (c) and in PVA (d). The solid lines show the fits to the data; the resulting redistribution times are noted for each trace.

at $\Delta\tau=0$. In addition to photobleaching, most of the dyes display characteristic "on–off" blinking. In our analysis of the SM2P data the on and off time windows were discriminated and only the on times were taken into account to deduce the ultrafast decay times. The fits are shown in Fig. 9. The uncertainty in the fit was determined by running Monte Carlo simulations using the redistribution time and the number of counts as found in the experimental trace. Since the times recovered are in general comparable or longer than the pulse length, the uncertainty in the fit is still reasonable even with the reduced number of detected photons.

From the data shown in Fig. 9 it appears that also these systems display a large variation in the redistribution times recovered. However, a larger number of molecules has to be studied in order to draw definite conclusions on the effect of the matrix and the range of distribution times exhibited by Cy3.5 and Atto590. On the other hand, our results confirm that the SM2P method can be used on less-photostable systems. The average power of a few kW/cm^2 used in these experiments is comparable to the powers used in standard single-molecule experiments. The increased peak power with respect to CW excitation results only in a slightly ($\sim$2 times) increased chance of photodissociation. Selected molecules can still be followed for a sufficient period to recover multiple SM2P dips. Moreover, on–off blinking is not a problem as long as one is able to distinguish the time intervals when the molecule is in the fluorescent state.

VIII. CONCLUSIONS

We have presented in detail a new experimental scheme that allows the detection of femtosecond processes in single molecules. The intramolecular energy redistribution time has been studied at different excitation energies and in different polymer matrices. Large variations in the redistribution time have been found from molecule to molecule. This effect has been attributed to an intramolecular process, since we did not find a dependence on matrix nor excitation wavelength. The variations in the redistribution times are most probably due to molecular conformational differences induced by the nanoenvironment surrounding the molecule.

Example traces were presented on two less-photostable molecules, demonstrating that the new SM2P technique is applicable to a broad range of systems. The SM2P technique can be readily extended to incorporate a second pulse of longer wavelength, allowing the study of ultrafast excitation energy flow through the vibrational ladder. This extension will open the door to the study of a wide variety of ultrafast processes at the level of single molecules.

ACKNOWLEDGMENTS

The authors thank Rudo Bouwhuis and Nan van Wijngaarden for initial experiments, Kobus Kuipers for fruitful discussions, and Jeroen Korterik for experimental support. We furthermore thank J. García-López for the perylene samples. This work was part of the research program 42 "Single molecule detection and nano-optics" of the Stichting voor Fundamenteel Onderzoek der Materie [FOM, financially supported by the Nederlandse Organisatie voor Wetenschappelijk Onderzoek (NWO)]. One of the authors (J.H.) thanks the EC Program IHP-99 for a Marie Curie Fellowship (HPMF-CT-2002-01698).

[1] R. van Grondelle and V. Novoderezhkin, Biochemistry **40**, 15057 (2001).
[2] J. L. Herek, W. Wohlleben, R. J. Cogdell, D. Zeidler, and M. Motzkus, Nature (London) **417**, 533 (2002).
[3] J. Yu, D. Hu, and P. F. Barbara, Science **289**, 1327 (2000).
[4] J. S. Baskin, H. Z. Yu, and A. H. Zewail, J. Phys. Chem. A **106**, 9837 (2002).
[5] R. M. Stratt and M. Maroncelli, J. Phys. Chem. **100**, 12981 (1996).
[6] W. P. D. Boeij, M. S. Pshenichnikov, and D. A. Wiersma, Annu. Rev. Phys. Chem. **49**, 99 (1998).
[7] S. Woutersen and H. J. Bakker, Nature (London) **402**, 507 (1999).
[8] S. Völker, Annu. Rev. Phys. Chem. **40**, 499 (1989).
[9] M. Dantus, R. M. Bowman, and A. H. Zewail, Nature (London) **343**, 737 (1990).
[10] D. J. Nesbitt and R. W. Field, J. Phys. Chem. **100**, 12735 (1996).
[11] S. A. McKinney, A. C. Declais, D. M. J. Lilley, and T. Ha, Nat. Struct. Biol. **10**, 93 (2003).
[12] W. E. Moerner and L. Kador, Phys. Rev. Lett. **62**, 2535 (1989).
[13] M. Orrit and J. Bernard, Phys. Rev. Lett. **65**, 2716 (1990).
[14] E. Betzig and R. J. Chichester, Science **262**, 1422 (1993).
[15] H. Gersen, M. F. García-Parajó, L. Novotny, J. A. Veerman, L. Kuipers, and N. F. van Hulst, Phys. Rev. Lett. **85**, 5312 (2000).
[16] T. Basché, S. Kummer, and C. Brauchle, Nature (London) **373**, 132 (1995).
[17] D. A. Higgins and P. F. Barbara, J. Phys. Chem. **99**, 3 (1995).
[18] S. Kummer, S. Mais, and T. Basché, J. Phys. Chem. **99**, 17078 (1995).
[19] M. Vogel, A. Gruber, J. Wrachtrup, and C. Vonborczyskowski, J. Phys. Chem. **99**, 14915 (1995).
[20] J. J. Macklin, J. K. Trautman, T. D. Harris, and L. E. Brus, Science **272**, 255 (1996).
[21] P. Tinnefeld, K. D. Weston, T. Vosch *et al.*, J. Am. Chem. Soc. **124**, 14310 (2002).
[22] B. Hecht, Philos. Trans. R. Soc. London, Ser. A **362**, 881 (2004).
[23] P. Tamarat, A. Maali, B. Lounis, and M. Orrit, J. Phys. Chem. A **104**, 1 (2000).
[24] W. E. Moerner, J. Phys. Chem. B **106**, 910 (2002).
[25] J. Hofkens, T. Vosch, M. Maus *et al.*, Chem. Phys. Lett. **333**, 255 (2001).

[26] R. A. L. Vallée, N. Tomczak, L. Kuipers, G. J. Vancso, and N. F. van Hulst, Phys. Rev. Lett. **91**, 038301 (2003).
[27] R. Zondervan, F. Kulzer, S. B. Orlinskii, and M. Orrit, J. Phys. Chem. A **107**, 6770 (2003).
[28] R. A. L. Vallée, M. Cotlet, M. van der Auweraer, J. Hofkens, K. Müllen, and F. C. de Schryver, J. Am. Chem. Soc. **126**, 2296 (2004).
[29] A. Kusumi, Y. Sako, and M. Yamamoto, Biophys. J. **65**, 2021 (1993).
[30] T. Funatsu, Y. Harada, M. Tokunaga, K. Saito, and T. Yanagida, Nature (London) **374**, 555 (1995).
[31] A. M. van Oijen, M. Ketelaars, J. Kohler, T. J. Aartsma, and J. Schmidt, Science **285**, 400 (1999).
[32] S. Weiss, Science **283**, 1676 (1999).
[33] M. F. Garcia-Parajo, G. M. J. Segers-Nolten, J. A. Veerman, J. Greve, and N. F. van Hulst, Proc. Natl. Acad. Sci. U.S.A. **97**, 7237 (2000).
[34] L. Cognet, C. Tardin, D. Boyer, D. Choquet, P. Tamarat, and B. Lounis, Proc. Natl. Acad. Sci. U.S.A. **100**, 11350 (2003).
[35] T. M. Jovin, Nat. Biotechnol. **21**, 32 (2003).
[36] A. Yildiz, J. N. Forkey, S. A. McKinney, T. Ha, Y. E. Goldman, and P. R. Selvin, Science **300**, 2061 (2003).
[37] A. Yildiz, M. Tomishige, R. D. Vale, and P. R. Selvin, Science **303**, 676 (2004).
[38] T. Unold, K. Mueller, C. Lienau, T. Elsaesser, and A. D. Wieck, Phys. Rev. Lett. **92**, 157401 (2004).
[39] M. Dyba and S. Hell, Phys. Rev. Lett. **88**, 163901 (2002).
[40] L. Kastrup and S. Hell, Angew. Chem., Int. Ed. **43**, 6646 (2004).
[41] E. M. H. P. van Dijk, J. Hernando, J. García-López, M. Crego-Calama, D. N. Reinhoudt, L. Kuipers, M. F. García-Parajó, and N. F. van Hulst, Phys. Rev. Lett. **94**, 078302 (2005).
[42] J. Cao, C. J. Bardeen, and K. R. Wilson, Phys. Rev. Lett. **80**, 1406 (1998).
[43] M. Orrit, Single Mol. **3**, 255 (2002).
[44] J. Y. Liu, W. H. Fan, K. L. Han, D. L. Xu, and N. Q. Lou, J. Phys. Chem. A **107**, 1914 (2003).
[45] M. J. Rosker, F. W. Wise, and C. L. Tang, Phys. Rev. Lett. **57**, 321 (1986).
[46] J. Y. Liu, W. H. Fan, K. L. Han, W. Q. Deng, D. L. Xu, and N. Q. Lou, J. Phys. Chem. A **107**, 10857 (2003).
[47] J. T. Fourkas and M. Berg, J. Chem. Phys. **98**, 7773 (1993).
[48] B. Bagchia, J. Chem. Phys. **100**, 6658 (1994).
[49] K. D. Weston, P. J. Carson, H. Metiu, and S. K. Buratto, J. Chem. Phys. **109**, 7474 (1998).